J. CHEM. SOC. FARADAY TRANS., 1995, 91(11), 1571–1585

Rotational Isomerism in Acrylic Acid

A Combined Matrix-isolated IR, Raman and *ab initio* Molecular Orbital Study

Anatoly Kulbida
Institute of Physics, St. Petersburg University, Peterhof, 198904 St. Petersburg, Russia
Mozart N. Ramos
Departamento de Química Fundamental, Universidade Federal de Pernambuco, Recife-PE, Brazil
Markku Rasanen and Janne Nieminen
Department of Physical Chemistry, P.O. Box 55, (A.I. Virtanens Square 1), 00014 University of Helsinki, Finland
Otto Schrems
Alfred-Wegener Institut fur Polar und Meeresforschung, Postfach 120161, D-27515 Bremerhaven, Germany
Rui Fausto*
Departamento de Química, Universidade de Coimbra, P-3049 COIMBRA, Portugal

The results of a combined vibrational and structural study of the acrylic acid monomer undertaken by matrix-isolated low-temperature IR spectroscopy and *ab initio* SCF-HF and MP2 MO calculations are presented. In addition, both Raman and IR spectra of liquid acrylic acid and the Raman spectrum of the crystal are also reported and interpreted. It is shown that in both argon and krypton matrices acrylic acid monomer exists as a mixture of two conformers of similar energies, differing by the relative orientation of the C=C—C=O axis. Upon irradiation at $\lambda = 243$ nm by a xenon lamp, the *s-cis* form (C=C—C=O dihedral angle equal to 0°), corresponding to the conformational ground state, converts to the *s-trans* form (C=C—C=O dihedral angle equal to 180°). In the liquid phase, dimeric structures strongly predominate, but the existence in this phase of the two conformational states referred to above can also be inferred from the corresponding vibrational spectra. In turn, in the crystal only the thermodynamically most stable form (*s-cis*) exists. Results of *ab initio* SCF-HF and MP2 molecular orbital (MO) calculations, in particular optimised geometries, relative stabilities, dipole moments and harmonic force fields, for the relevant conformational states of acrylic acid are also presented and the conformational dependence of some relevant structural parameters is used to characterise the most important intramolecular interactions present in the studied conformers. Finally, the calculated vibrational spectra and both the results of a normal-mode analysis based on the theoretical harmonic force fields and of IR intensity studies based on the charge–charge flux–overlap (CCFO) model were used to help interpret the experimental vibrational data, enabling a detailed assignment of the acrylic acid spectra obtained in the different conditions considered.

Acrylic-based materials (polymers) have a wide range of practical commercial applications and have been widely studied.[1–3] However, despite the relevance of these systems, to date their precursors (monomers) have neither been studied systematically in detail or characterised well, either structurally or spectroscopically. In addition, acrylic-like molecules have also been proved to be of fundamental importance to the study of some catalytic reactions involving serine proteases (*e.g.* chymotrypsin),[4–6] since they can be successfully used as *in situ* resonance Raman spectroscopic probes of the enzyme–substrate transient complexes formed within the enzyme's active site during catalysis.[4,5] Indeed, in this field of research, a detailed knowledge of both conformational preferences and vibrational properties of simple molecules containing the acrylyl moiety assumes particular relevance, as stressed elsewhere.[4,5]

Among the simplest molecules containing the acrylyl fragment, acrylic acid monomer naturally appears as one of the most fundamental systems to be studied, but it also represents a challenge to fundamental research owing to the practical difficulty of avoiding its polymerisation under current experimental conditions.[7] This may explain why neither the precise molecular structure nor the vibrational spectra of the monomeric acrylic acid have been reported, though several studies have already looked at its dimeric structures.[7–12]

To the best of our knowledge, besides an earlier electron diffraction study in which the conformational isomerism was not analysed,[13] only a few more recent structural and/or vibrational experimental studies on monomeric acrylic acid have been reported. In a first study, the microwave spectrum of acrylic acid was analysed, and two different conformers differing in the relative position of the acrylyl group were found to exist in the gaseous phase (the *s-cis* and *s-trans* forms; Fig. 1).[14] In that study, however, a unique set of assumed geometrical parameters taken from related molecules was used to describe the structure of both conformers. Thus, it was not possible to analyse the influence of the conformation on the molecular geometry and, consequently, also to determine, from the conformational dependence of the geometrical parameters, which are the main factors responsible for the relative stability of the observed conformers. A second study used the semiempirical Neglect of Diatomic Differential Overlap (NDDO) method to investigate the conformational stabilities, dipole moments and ionisation potentials of the two most stable conformers of acrylic acid.[15] Reasonable agreement between the calculated and available experimental data could be reached, despite the low theoretical level of the calculations undertaken. A more recent study considered the structures of acrylic acid and complexes of this molecule with Lewis acids (*e.g.* H^+, Li^+, BH_3), in order to rationalize the stereoselectivity of catalysed Diels-Alder reactions of chiral acrylates.[16] SCF-HF calculations, undertaken using both the 3-21G and 6-31G* basis sets at the 3-21G optimised geometries, confirmed the slightly lower energy of the *s-cis* conformer of acrylic acid

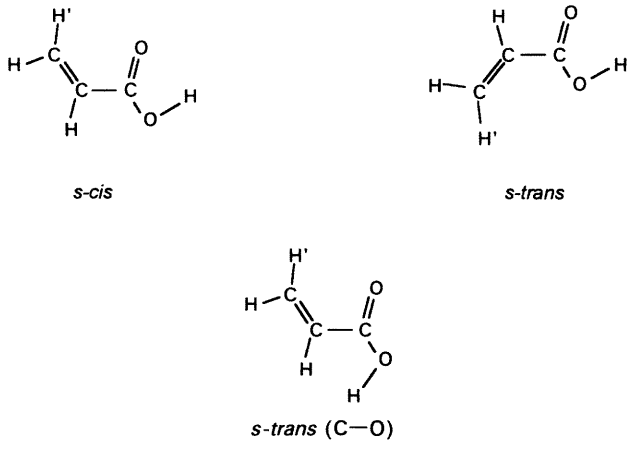

Fig. 1 Conformers of acrylic acid (monomer)

[$\Delta E_{(s\text{-}trans)-(s\text{-}cis)}$ = 2.86 kJ mol^{-1} (3-21G); 2.51 kJ mol^{-1} (6-31G* and 3-21G)]. However, no geometry optimisation was carried out at the highest level of calculations used (SCF-HF 6-31G*), and electron correlation effects were not analysed. In addition, in that study, no vibrational studies were undertaken.[16] Finally, the latest study concerned the matrix-isolated spectra of acrylic acid at 25 K,[17] and was complemented by a theoretical study carried out at the SCF-HF 4-21G level.[18] In these last studies, based both on the different intensity behaviour of the observed bands upon sample irradiation by UV light obtained from a medium pressure mercury lamp and on the comparison between the observed and calculated spectra, an assignment of the observed bands to the *s-cis* and *s-trans* conformers was proposed. Although these studies have greatly improved our knowledge of the acrylic acid monomer structural and vibrational properties, the results obtained in the earlier studies could not answer some important questions:

(i) First, it was not possible to separate clearly the spectra of the two observed conformers and, thus, some of the assignments made in ref. 17 were only tentative;

(ii) The force field scaling used to fit the calculated spectra to the experimental frequencies was made by transferring different scale factors previously obtained for other molecules.[18,19] However, the use of several scaling factors may lead to significant changes in the potential-energy distribution (PED), thus often introducing undesirable *a posteriori* distortions in the force fields. The method of transferring the scale factors from different molecules naturally strongly increases the probability of obtaining physically meaningless results. Moreover, the theoretical results were obtained at the SCF-HF 4-21G level,[18] and it is nowadays well known that, for systems containing conjugated double bonds, reliable structural and vibrational results can in general only be achieved if at least polarisation functions on all non-hydrogen atoms are added to the basis set;[20,21]

(iii) Finally, no discussion was presented concerning both the differences in the molecular geometries of the two conformers studied and the factors which may explain their relative stability, and no attempt was made to correlate the relevant geometrical parameters with either vibrational frequencies or intensities.

In this work, considering all the open questions above, the molecular structure and vibrational properties of acrylic acid conformers have been studied using a more systematic and precise approach. Since matrix-isolation spectroscopy provides a unique way of studying the monomer of acrylic acid, this technique was used to obtain the IR spectrum of the molecule and to study the rotamerization processes taking place upon sample irradiation by UV light at $\lambda = 243$ nm. To help interpret the experimental data, a series of SCF-HF and MP2 *ab initio* molecular orbital calculations have been performed using both the 6-31G* and 6-311 + G** basis sets which include, respectively, one set of polarisation functions in all non-hydrogen atoms and polarisation functions in all atoms plus one set of diffuse functions in non-hydrogen atoms. Besides the molecular structures and relative energies of the various stable conformations, theoretical calculations of the vibrational spectra of the individual conformers have also been carried out, providing us with very valuable information for the assignment of the experimental spectra. These results are complemented by normal-mode calculations based on the SCF-HF 6-31G* theoretical harmonic force fields and by IR intensity studies based on the CCFO model.[22] Finally, the experimental vibrational spectra (Raman and IR) of acrylic acid in both liquid and crystalline phases are reviewed considering the results obtained for the isolated molecule.

Experimental and Computational Methods

Acrylic acid (99 + % purity) was obtained from Fluka and purified by several freeze–pump–thaw cycles. Ar and Kr were obtained from Messer Griesheim GmbH and had, respectively, 99.999% and 99.998% purity. All matrices were prepared in a conventional way by deposition of the gaseous mixture on a gold-plated copper mirror, cooled using an ROK 10–300 (Leybold-Heraeus) closed-cycle refrigerator. The deposition temperatures, measured at the mirror with a silicon diode and a DRC 93C temperature controller (Lake Shore Cryotonics) were 14 or 18 K (Ar) and 25 K (Kr). The matrix : solute ratios were *ca.* 1500 : 1 and the rates of the matrix gas flow *ca.* 5.0 × 10^{-3} (Ar) or 1.5 × 10^{-3} (Kr) mol h^{-1}. Further details on the sample preparation procedure can be found in ref. 23.

The IR spectra were recorded in the reflection mode (0.5 cm^{-1} resolution) on a Bruker IFS 66 V Fourier transform spectrometer equipped with a germanium on CsI beam splitter and with a DTGS detector with CsI windows. The irradiation of the samples was carried out using a UV-light source (L.O.T.-Oriel GmbH) whose main component is a 500 W Xe arc lamp. The collimated UV beam irradiated the sample through the Suprasil window of the cryostat after being filtered by both a water filter and interference filter of the FS10–50 type with a bandwidth of *ca.* 8–10 nm (L.O.T.-Oriel GmbH).

Raman spectra were obtained using a SPEX 1403 double monochromator spectrometer (focal distance 0.85 m, aperture *f*/7.8), equipped with holographic gratings with 1800 grooves mm^{-1} (1800-1SHD). The 514.5 nm argon laser (Spectra-Physics, model 164-05) line, adjusted to provide 220 mW power at the sample, was used as the exciting radiation. Detection was effected using a thermoelectrically cooled Hamamatsu R928 photomultiplier. Spectra were recorded using increments of 1 cm^{-1} and integration times of 1 s. Under these conditions, the estimated errors in wavenumbers are ±1 cm^{-1}.

The *ab initio* SCF-HF and MP2 MO calculations were carried out with both the 6-31G* and 6-311 + G** basis sets,[24,25] using the GAUSSIAN92 program system.[26] The 6-31G* calculations were performed on a DEC ALPHA 7000 computer, at the Centre of Informatics of the University of Coimbra (CIUC), Portugal, while the 6-311 + G** calculations were carried out on CRAY-X MP/EA 432 and on CONVEX C3840 computers at the Centre for Scientific Calculations, Espoo, Finland. Molecular geometries were fully optimised by the force gradient method using Berny's algo-

rithm.[27] The largest residual internal coordinate forces were always less than 3×10^{-4} E_h a_0^{-1} or E_h rad^{-1}, for bond stretches and angle bends, respectively.† The force constants (symmetry internal coordinates) to be used in the normal coordinate analysis were obtained from the *ab initio* cartesian harmonic force constants using the program TRANSFORMER.[28] This program was also used to prepare the input data for the normal coordinate analysis programs used in this study (BUILD-G and VIBRAT[29]). The calculated force fields were then scaled down by using a simple linear regression for each symmetry class in order to adjust the calculated to the experimental frequencies (two scale factors are obtained: one related to the in-plane vibrations, and the other to the out-of-plane modes). Unobserved bands (or bands doubtfully ascribable using only a pure empirical approach) were then calculated from the corresponding force fields by interpolation using the straight lines obtained previously. While very simple, this scaling procedure preserves the PEDs as they emerge from the *ab initio* calculations, thus having an important advantage over the more elaborate force field scaling procedures which use more than one scale factor for each symmetry class which usually give rise to important PEDs distortions from the *ab initio* calculated values.

IR intensity parameters were examined using the atomic polar tensor (APT) formalism[30] and the CCFO model.[22,31]

Results and Discussion

Geometries and Energies

Several acrylic acid derivatives of general formula $H_2C{=}CHC(=O)X$, including acrolein,[18,32,33] methyl vinyl ketone,[34] acrylyl halides[35–38] and methyl acrylate,[39,40] have been the subject of detailed structural and vibrational studies, and it has been shown that the relative order of stability of the *s-cis* and *s-trans* conformers is strongly determined by the nature of the substituent, X, bound to the carbonyl carbon atom. In fact, the relative $\Delta E_{(s\text{-}trans)-(s\text{-}cis)}$ values shown in Table 1 for a series of acrylic acid derivatives can be interpreted by considering that when conjugation is possible between the carbonyl and the X substituent (canonical form II in Fig. 2), the *s-cis* conformer is considerably stabilised relative to the *s-trans* form. This justifies the relative values observed for the halides, where the extent of the conjugation between the halogen and the carbon atoms follows the well known order F > Cl > Br. Moreover, the results point also to a particularly important *s-cis* stabilisation in carboxylic compounds. On the other hand, the greater importance of the mesomerism within the C=C—C=O moiety (canonical form III in Fig. 2) in the *s-trans* form may explain the greater stability of this conformation in molecules, such as aldehydes and ketones,[4,32–34] where mesomerism involving the X group is absent.

Table 1 $\Delta E_{(s\text{-}trans)-(s\text{-}cis)}$ (kJ mol^{-1}) for several molecules of general formula $H_2C{=}CHC(=O)X$

molecule	ΔE^a	ref.
$H_2C{=}CHC(=O)H$	−6.99	33
$H_2C{=}CHC(=O)CH_3$	−4.48	34
$H_2C{=}CHC(=O)Br$	−1.89	38
$H_2C{=}CHC(=O)Cl$	−1.76	38
$H_2C{=}CHC(=O)F$	0.95	38
$H_2C{=}CHC(=O)OCH_3$	2.40	40
$H_2C{=}CHC(=O)OH$	1.95	this work

[a] Results from SCF-HF *ab initio* calculations carried out at the split valence or split valence plus polarisation levels of theory.

† 1 E_h a_0^{-1} ≈ 8.238 73 × 10^{-8} N.

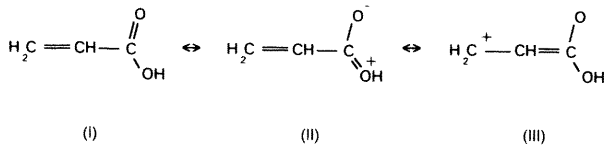

Fig. 2 Canonical forms of acrylic acid showing (II) mesomerism within the carboxylate group and (III) mesomerism associated with the two double bonds

Table 2 shows the calculated molecular geometries, rotational constants and energies for the various possible conformers of acrylic acid. At the SCF-HF level of theory, the *s-cis* form is predicted to be more stable than the *s-trans* conformer by 1.95 and 1.09 kJ mol^{-1}, respectively, using the 6-31G* and the 6-311 + G** basis sets (the corresponding $\Delta E_{(s\text{-}trans)-(s\text{-}cis)}$ values corrected by zero-point vibrational energies reduce slightly to 1.86 and 1.03 kJ mol^{-1}). The calculations carried out at the MP2 level of theory yield slightly higher $\Delta E_{(s\text{-}trans)-(s\text{-}cis)}$ values than those undertaken at the SCF-HF level (MP2/6-31G*: 2.81 kJ mol^{-1}; MP2/6-311 + G** at the SCF-HF/6-311 + G** optimised geometries: 1.51 kJ mol^{-1}), thus indicating that electron correlation effects tend to favour slightly the *s-cis* conformer. These calculated values compare fairly well with the previously obtained microwave result (0.60 ± 0.24 kJ mol^{-1} [14]) and are also the same order of magnitude as the conformer energy difference found for methyl acrylate (2.40 kJ mol^{-1}; *ab initio* SCF-HF/4-31G* [40]). Taking into consideration the comparable SCF-HF data, the slightly lower values found for acrylic acid when compared with those obtained for methyl acrylate can be explained by considering that the *s-cis* stabilisation due to the mesomerism within the C(=O)OX (X = H, CH_3) fragment is more important in the ester than in the acid, owing to the additional electron charge release from the methyl group towards the ester oxygen atom.

Note that the proposed relative importance in the two conformers of the stabilising intramolecular interactions due to (i) mesomerism involving the carboxylate group (which favours the *s-cis* form) and (ii) mesomerism within the C=C—C=O fragment (which favours the *s-trans* form) is consistent with the geometrical changes observed upon conformer interconversion. Thus, the C—O bond is shorter in the *s-cis* than in the *s-trans* form, while the C—C bond is longer, clearly showing that canonical form II of Fig. 2 is more important in the *s-cis* conformer and canonical form III is more important in the *s-trans* form.

The calculated changes in C—C=O, C—C—O, C=C—C, H—C—C and H′—C=C angles with conformation reveal the presence of stronger steric repulsions between the vinyl group and the carboxylic oxygen atom in the *s-trans* conformer, when compared with the vinyl–carbonyl interaction present in the *s-cis* form. In fact, the C—C=O and H—C—C angles decrease in going from the *s-cis* to the *s-trans* conformer, while the remaining angles increase. It is obvious that these changes, in particular those observed in the H—C—C and H′—C=C angles, constitute strong evidence indicating the greater importance of the CH_2=CH/—O— repulsions. More important steric repulsions between α-substituents and the —O— atom, compared with repulsions involving the carbonyl oxygen, have been previously found in other α-substituted carbonyl compounds[40–44] and seem to be a general structural trend which usually has important geometrical implications.

Table 2 Calculated optimised geometries, rotational constants, energies and electric dipole moments for the relevant forms of acrylic acid[a]

	s-cis			*s-trans*			*s-trans* (C—O)		
	SCF-HF		MP2	SCF-HF		MP2	SCF-HF		MP2
parameter	6-31G*	6-311 + G**	6-31G*	6-31G*	6-311 + G**	6-31G*	6-31G*	6-311 + G**	6-31G*
C=O	118.99	118.46	122.05	118.94	118.47	122.15	118.36	117.78	121.45
C—O	132.97	132.82	136.10	133.13	132.89	136.21	133.42	133.30	136.55
C—C	148.32	148.47	148.10	148.13	148.24	147.79	149.25	149.43	149.23
C=C	131.89	131.91	133.87	131.97	131.96	133.96	131.89	131.89	133.82
C_α—H	107.38	107.42	108.50	107.38	107.42	108.52	107.73	107.75	108.83
C_β—H	107.45	107.53	108.52	107.48	107.55	108.40	107.44	107.52	108.54
C_β—H′	107.42	107.53	108.44	107.36	107.44	108.50	107.40	107.51	108.44
O—H	95.21	94.59	97.95	95.18	94.56	97.89	94.72	94.12	97.37
O=C—O	122.43	122.56	122.84	122.30	122.38	122.57	120.46	120.54	120.00
C—C=O	125.77	125.75	126.20	123.63	123.47	124.16	123.94	124.03	124.29
C—C—O	111.80	111.69	110.96	114.07	114.15	113.27	115.60	115.43	
H—C—C	116.87	116.85	117.42	113.86	113.85	114.24	118.57	118.47	119.83
C=C—C	120.54	120.65	119.98	123.92	123.93	123.73	120.54	120.67	119.44
H—C=C	121.49	121.22	121.63	120.97	120.76	120.92	121.58	121.31	119.91
H′—C=C	120.88	120.87	120.29	121.88	121.74	121.52	120.57	120.60	121.74
C—O—H	108.12	108.74	105.50	107.73	108.44	105.01	112.44	112.43	109.97
C—C(=O)—O	180.00	180.00	180.00	180.00	180.00	180.00	180.00	180.00	180.00
H—C—C=O	180.00	180.00	180.00	0.00	0.00	0.00	180.00	180.00	180.00
C=C—C=O	0.00	0.00	0.00	180.00	180.00	180.00	0.00	0.00	0.00
H—C=C—C	180.00	180.00	180.00	180.00	180.00	180.00	180.00	180.00	180.00
H′—C=C—C	0.00	0.00	0.00	0.00	0.00	0.00	0.00	0.00	0.00
O=C—O—H	0.00	0.00	0.00	0.00	0.00	0.00	180.00	180.00	180.00
A	11 442.80 11078.80[b]	11484.18	10913.58	11032.77 10716.11[b]	11047.66	10672.38	11195.10	11237.43	10775.19
B	4302.23 4251.94[b]	4301.50	4253.96	4435.62 4388.28[b]	4443.37	4361.47	4328.34	4326.37	4256.25
C	3126.67 3073.39[b]	3129.37	3060.88	3163.69 3114.31[b]	3168.85	3096.16	3121.48	3123.74	3051.07
ΔE[c]	—	—	—	1.946	1.088	2.807	31.20	29.08	30.78
	—	—	—	(1.860)	(1.028)		(29.96)	(27.79)	
$\lvert\mu\rvert$	1.636 146 ± 0.10[b]	1.718	1.745	2.376 2.02 ± 0.05[b]	2.489	2.524	4.763	4.846	4.978

[a] Bond lengths in pm, angles in degrees, rotational constants in MHz, energies in kJ mol^{-1}, dipole moments in D. [b] Experimental value obtained by microwave spectroscopy.[14] [c] Relative energies to the most stable conformer, values presented in parentheses are relative energies including zero-point vibrational energy corrections. The total energies for the most stable *s-cis* form calculated with the 6-31G* and 6-311 + G** basis sets are, respectively, −265.654 347 1 and −265.734 924 2 E_h. The total energy for this conformer calculated at the MP2/6-31G* level is −266.380 565 5 E_h. MP2/6-311 + G** calculations performed at the optimised geometries obtained at the SCF-HF level using the same basis set yield $\Delta E_{(s\text{-}trans)-(s\text{-}cis)} = 1.514$ kJ mol^{-1} and $\Delta E_{[s\text{-}trans(C-O)]-(s\text{-}cis)} = 26.27$ kJ mol^{-1}.

In summary, the principal factors which determine the relative stability of the *s-cis* and *s-trans* conformers of acrylic acid are (i) mesomerism within the carboxylate group (canonical form II in Fig. 2), (ii) mesomerism involving both C=C and C=O double bonds (canonical form III in Fig. 2) and (iii) steric repulsions between CH_2=CH and the oxygen atoms. The first factor is the most important and, together with the third, favours the *s-cis* conformer; the second factor favours the *s-trans* conformer. On the whole, these interactions make the *s-cis* form more stable than the *s-trans* conformer.

The SCF-HF/6-31G* calculated potential-energy profile for internal rotation about the C—C bond is shown in Fig. 3, together with the results of the quantitative potential-energy deconvolution

$$V = V^\circ + \frac{1}{2}\sum_{n=1,3} V_n[1 - \cos(n\tau)]$$

where τ is the C=C—C=O dihedral angle and V° is the energy corresponding to a C=C—C=O angle of 0°.

The calculated energy barrier amounts to 30.4 kJ mol^{-1}, and corresponds to a C=C—C=O dihedral angle of 92.4°. The corresponding experimental values are 16.0 ± 6.0 kJ mol^{-1} and $89 \pm 4°$.[14] Thus, the SCF-HF *ab initio* calculations considerably overestimate the energy barrier, a result which follows the trend previously observed for other molecules which also exhibit conformational isomerism about partial double bonds.[42–45] In order to evaluate the importance of electron correlation on the calculated energy barrier, MP2/6-31G* calculations were also carried out for the rotational transition state. The calculated energy barrier amounts to 26.9 kJ mol^{-1}, an improvement over the results obtained at the SCF-HF level of theory.

Comparison of the calculated structural data given in Table 2 shows that similar results are obtained at the SCF-HF level of theory using the 6-31G* and 6-311 + G** basis sets. This leads, for instance, to identical calculated rotational constants which, in turn, when compared with the available experimental data obtained by microwave spectroscopy[14] show rather large differences. On the other hand, the MP2/6-31G* optimised structures are clearly different from those obtained at the SCF-HF level, and lead to rotational constants that show a very good agreement with the experimental data. Besides the C—H bond lengths, which are calculated to be *ca.* 1 pm longer at the MP2 level, the main differences between the MP2 and SCF-HF geometries occur for the C=O, C—O, C=C and O—H bond lengths (which are calculated, respectively, to be *ca.* 3, 3, 2 and 3 pm longer at the MP2 level) and for the C—O—H angles (which decrease by 2–3° when electron correlation effects are considered).

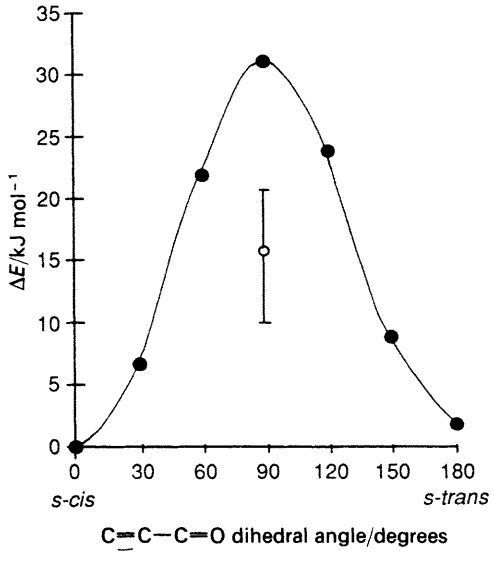

Fig. 3 SCF-HF/6-31G* optimised conformational energy profile for internal rotation about the C—C bond of acrylic acid (O=C—O—H axis in the *s-cis* conformation). The energy components resulting from the quantitative potential-energy deconvolution, $V = V^\circ + \frac{1}{2}\sum_{n=1,3} V_n[1 - \cos(n\tau)]$, where τ is the C=C—C=O dihedral angle and V° is the energy corresponding to a C=C—C=O angle of 0°, are $V_1 = 2.43$, $V_2 = 29.60$ and $V_3 = -0.81$ kJ mol^{-1}. The unfilled circle represents experimental data.[14]

Acrylic acid monomer possesses an additional degree of conformational freedom, which is related to the internal rotation about the C—O single bond. In general, carboxylic acids adopt the *s-cis* conformation about this bond (O=C—O—H dihedral angle equal to 0°), the energy difference between this conformation and that of the second stable form (the *s-trans* conformer, corresponding to an O=C—O—H dihedral angle equal to 180 °C) and the energy barrier for interconversion between these two forms usually being very large (over 20 and 40 kJ mol^{-1}, respectively[42–45]). The main factor which determines the much lower energy of the *s-cis* O=C—O—H axis when compared with that of the *s-trans* O=C—O—H axis is the presence in the latter of the strongly stabilising through-space field interaction resulting from the nearly antiparallel alignment of the C=O and O—H bond dipoles.[42] In general, *s-trans* (C—O) conformers are not observed spectroscopically under the present experimental conditions, unless particular specific intramolecular stabilising interactions are operating (as, for instance, intramolecular hydrogen bonding in chloroacetic acid monomer[23,46]). However, *s-trans* (C—O)-like conformations of α,β-unsaturated carbonyls have been recently proposed as catalytically important conformational states,[47] thus justifying the interest in studying *s-trans* (C—O) conformational states of acrylic acid as well. For this molecule, the energy difference between the single *s-trans* (C—O) conformer predicted by the SCF-HF calculations (in this conformer the C=C—C=O axis adopts the *s-cis* conformation; see Fig. 1) and the most stable conformer (*s-cis*), calculated using the 6-31G* and 6-311 + G** basis sets amounts, respectively, to 31.20 and 29.08 kJ mol^{-1} (if the zero-point vibrational energy corrections are considered, the calculated values are reduced to 29.96 and 27.79 kJ mol^{-1}). Consideration of electron correlation does not significantly affect this energy difference, though slightly lower values were obtained (MP2/6-31G*: 30.78 kJ mol^{-1}; MP2/6-311 + G** at the SCF-HF/6-311 + G** optimised geometries: 26.27 kJ mol^{-1}). Note that, as previously found for methyl acrylate,[40,48] the *s-trans* (C—C)/*s-trans* (C—O) conformation was not found to correspond to a minimum in the potential-energy surface of acrylic acid, pointing to the existence of very strong steric interactions between the carboxylic hydrogen atom and the vinyl group in this conformation.

By comparing the molecular geometries of the *s-trans* (C—O) form with those of the two *s-cis* (C—O) conformers (*s-cis* and *s-trans* forms) the following conclusions can also be drawn:

(i) The O—H bond is shorter in the *s-trans* (C—O) conformer than in the two *s-cis* (C—O) conformers. This is a direct consequence of the presence in these latter conformers of the above mentioned C=O···O—H through-space field interaction which leads to an increase in the O—H bond length by inducing an electronic charge migration from the overlap O—H region towards the —O— atom;

(ii) The C=O and C—O bond lengths are, respectively, smaller and larger than in the two *s-cis* (C—O) conformers,

indicating that the mesomerism within the carboxylate group has a reduced importance when the O=C—O—H axis assumes the *s-trans* conformation;

(iii) Though they are less strong than in the *s-trans* (C—C)/*s-trans* (C—O) conformation (which, as pointed out before, corresponds to a conformational transition state, saddle point) the OH···vinyl repulsive steric interactions are still very important in the *s-trans* (C—O) conformer (the C—C—O, C—O—H and H—C—C angles are very large in this form). They are not, however, strong enough to put the energy of the planar conformation above that of non-planar structures, where the mesomerism involving the C=C—C=O moiety and/or the carboxylic group cannot operate efficiently;

(iv) The OH···vinyl steric interactions are also responsible, at least in part, for the presence of a longer C—C bond in the *s-trans* (C—O) conformer, though this result may also be partially due to a reduced importance in this form of the mesomerism involving the C=C—C=O moiety.

In summary, it can be concluded from the structural data that all the four most important intramolecular interactions which determine the relative energies of the different conformations of acrylic acid [C=O···O—H bond dipolar (through-space field) interaction; mesomerism within the carboxylate group; mesomerism involving the C=C and C=O double bonds; vinyl···carboxylate steric repulsions] contribute to some extent to increasing the energy of the *s-trans* (C—O) conformer with respect to the most stable forms.

Charge Distribution Analysis

Fig. 4 presents values of standard (ζ_M) and corrected (ζ_{corr}) Mulliken atomic charges for the three isomers of acrylic acid, as calculated with the 6-31G* basis set, at the SCF-HF level.

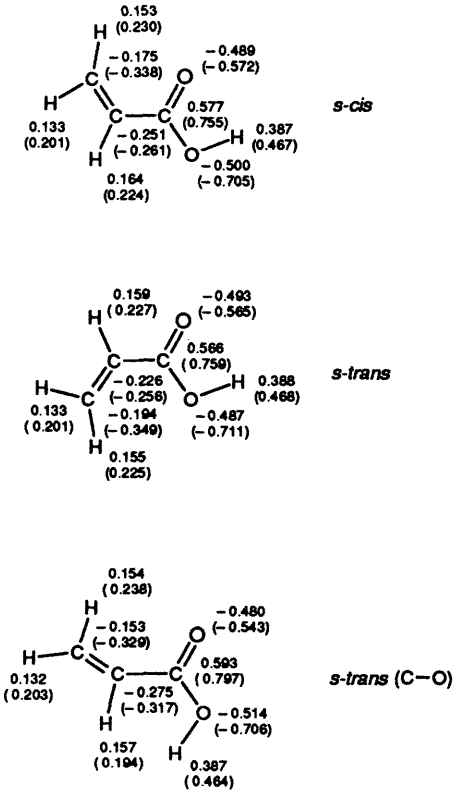

Fig. 4 SCF-HF/6-31G* calculated standard and corrected Mulliken atomic charges for the various conformers of acrylic acid. The standard values are given in parentheses.

The corrected Mulliken charges are given by

$$\zeta_{corr}(\alpha) = \zeta_M(\alpha) + \Delta^{xx}_{ov,\alpha}$$

where x is the cartesian axis perpendicular to the molecular plane, and $\Delta^{xx}_{ov,\alpha}$ is a specific element of the overlap tensor derived from the CCFO model for IR intensities,[22,31] in order to reproduce the SCF dipole moments from atomic charges.[49,50] It has been shown[49–52] that this correction is useful to reduce the large basis set dependence of Mulliken charges[53,54] and to improve the description of intramolecular interactions.

The atomic charge partitionings given by the corrected and standard Mulliken charges show important differences. In particular:

(i) The bonds involving all but the hydrogen atoms are predicted to be considerably less polarised when the corrected charges are considered, in particular the C—O single bond, whose associated bond-dipole moment is calculated to be *ca.* 3.5 D† when corrected Mulliken charges are used and *ca.* 4.8 D when standard Mulliken charges are considered.

(ii) The corrected atomic charges on the hydrogen atoms are considerably less positive than the corresponding standard charges. This feature has also been noted in other planar carbonyl and thiocarbonyl molecules [for example, HC(=X)YH; X, Y = O or S[52])], and thus appears to be a general rule for this kind of molecular system. The observed reduction of the hydrogen atomic charges upon correction amounts to *ca.* 0.07 *e* (1 *e* = 1.602 189 2 × 10^{-19} C), the range of values being 0.13–0.16 *e* and 0.20–0.24 *e*, for the corrected and standard Mulliken charges, respectively (see Fig. 4).

(iii) Upon correction, the polarity of the C=C bond is reversed in all conformers, the C_β atom becoming less negative than the C_α. Indeed, both carbon atoms reduce their negative charges, but this reduction is considerably more pronounced in the case of C_β. Thus, this result is a consequence of the above-mentioned general reduction of positive charges on hydrogens upon correction (C_β has two hydrogens, whilst C_α has just one hydrogen). However, the picture obtained using the corrected charges is the one which is consistent with the relevant importance of canonical form III of Fig. 2 (describing the mesomerism involving both the C=C and C=O double bonds) to the structure of the molecule. Very interestingly, the considerable reduction upon correction of the charge of the —O— atom in all conformers (much more pronounced than that of the carbonyl atom) leads to a charge distribution picture which is in much better agreement with a relevant contribution of canonical form II of Fig. 2 (representing the mesomerism within the carboxylate group) to the molecular structure of acrylic acid.

In general terms, it can be concluded that the standard Mulliken partitioning of charges overestimates the polarity of the various bonds, in particular those of the C—O bonds in all conformers. Since the IR intensities of well localised stretching vibrations in general increase with the polarisation of the associated bond,[55] it could then be expected that IR intensities predicted using the Mulliken standard charges would also show a general overestimation. In turn, as it will be stressed in the next section, the corrected charges can be successfully used to estimate the IR intensities of several important vibrations of acrylic acid.

Finally, it should be noted that the change in conformation does not produce large changes in the atomic charges. This is true for both standard and corrected charges (see Fig. 4), and is a very interesting result since, on the contrary, in some

† 1 D ≈ 3.335 64 × 10^{-30} C m.

cases, the intensities of the IR bands ascribable to the same normal mode in different conformers show remarkable differences (this is particularly evident in the case of stretching vibrations involving non-hydrogen atoms). Thus, the theoretical results indicate that the relative contribution of the charge-flux terms[55] to the total IR intensities of these bands are dominant. A systematic analysis of the importance of charge fluxes to the relative intensities of the IR bands associated with the most important normal modes originating in the various conformers of acrylic acid is presented in the next section.

Vibrational Studies

Assignment of Vibrational Spectra of the Monomer

The IR spectra of acrylic acid isolated in Ar and Kr matrices are essentially the same; the observed frequencies and intensities do not differ by more than 0.5%. The following discussion will therefore focus on the results obtained in the Ar matrix.

The IR spectrum of acrylic acid trapped in an Ar matrix at 18 K deposition temperature is shown in Fig. 5(*a*). In addition to the bands due to the monomers, the spectrum contains some low intensity bands due to traces of cyclic dimers initially present in the jet used to prepare the samples, which could be identified by recording the spectra with different matrix : solute ratios.

Under irradiation with UV light of decreasing wavelength, a noticeable redistribution of band intensities begins to take place at *ca.* 253 nm (filter 250FS10–50; peak transmission 19% at 253 nm; bandwidth 8.8 nm). Under irradiation in the 243 nm region (filter 240FS10–50; peak transmission 24% at 243 nm; bandwidth 9.4 nm), the changes were found to be several times faster than during the 253 nm irradiation, though weak traces of CO, CO_2 and H_2O appear in the spectrum, indicating the beginning of the acrylic acid photodissociation processes. Fig. 5(*b*) shows the differential spectrum after irradiation in the 243 nm region over 140 min (in hexane solution at room temperature, the λ_{max} of the acrylic acid absorption band is 223 nm, and the half bandwidth 30 nm; thus, the irradiation was carried out in the long-wave wing of the absorption band). The changes in the spectrum shown in Fig. 5(*b*) are close to the saturation point (except in the case of the bands due to the products of photodissociation, CO, CO_2 and H_2O, which were still slowly increasing in intensity). Under irradiation by non-filtered UV light, the observed changes in the spectrum were found to be the same, but the CO_2 : CO band intensity ratio increases from *ca.* 1 : 3 to close to unity. In turn, under irradiation by an ArF excimer laser (193 nm), the amount of CO_2 was found to be *ca.* 10 times higher than that of CO. The products of acrylic acid photodissociation could be, for example, $CH_2CH_2 + CO_2$ or $CHCH + H_2O + CO$, but no new bands have been observed except those corresponding to CO, CO_2 and H_2O. We are currently studying the photodecomposition of acrylic acid in matrices, including the product yield dependence on precursor conformation.

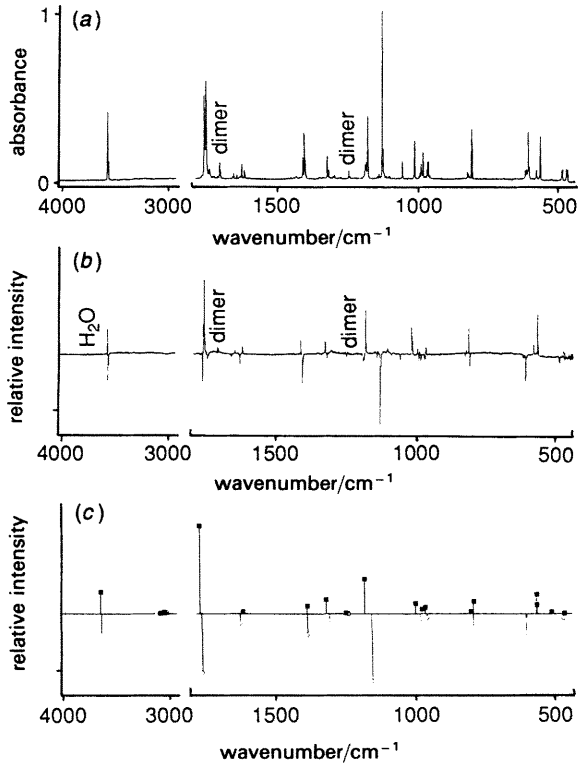

Fig. 5 (*a*) IR spectrum of acrylic acid isolated in an argon matrix after deposition at 18 K; (*b*) difference spectrum obtained by subtracting (*a*) from the spectrum obtained after UV-irradiation in the 243 nm region over 140 min [scales of (*a*) and (*b*) are related by a factor of three]; (*c*) SCF-HF/6-31G* calculated IR spectra of *s-cis* and *s-trans* conformers. In (*b*) and (*c*), the upwards going bands are due to the *s-trans* conformer while the downwards going bands originate from the *s-cis* form. Relative intensities in (*b*) and (*c*) correspond to normalised intensities to the most intense band (calculated) or group of bands (experimental) assigned to the ν(C=O) vibration in the *s-trans* form.

As the UV irradiation leads only to a redistribution of the intensities of the precursor bands already present in the spectrum (two sets of bands showing different behaviour upon irradiation were found) and, in particular, since no new bands could be observed, the observed changes must be due to a rotamerization reaction between the *s-cis* and *s-trans* conformers, the two forms being significantly populated at the deposition temperature. Indeed, as indicated by the calculations (see Table 2), the relative energy of the remaining conformer of acrylic acid [the *s-trans* (C—O) form] is high enough to avoid this form being significantly populated even at considerably high temperatures. The comparison between the difference spectra shown in Fig. 5(*b*) and the calculated spectra [Fig. 5(*c*)] unequivocally proves that the upwards bands originate in the *s-trans* conformer, while the downwards bands are due to the *s-cis* form and, thus, that irradiation promotes (*s-cis*) → (*s-trans*) isomerization.

Considering the ratio of the *s-cis* and *s-trans* rotamer absorption coefficients taken from the differential spectrum [Fig. 5(*b*)], it can be estimated from the spectrum shown in Fig. 5(*a*) that the (*s-cis*)/(*s-trans*) concentration ratio in the non-irradiated sample is *ca.* 1.4. Thus, assuming that the concentration ratio did not change appreciably during the deposition process, this value leads to an estimate of $\Delta E_{(s\text{-}trans)-(s\text{-}cis)}$ of *ca.* 0.8 kJ mol^{-1}, which is in good agreement with the energy difference found in the gaseous phase by microwave spectroscopy (0.60 ± 0.24 kJ mol^{-1} [14]). On the other hand, since the annealing of the matrices up to 32 K does not change the spectra of either irradiated or non-irradiated samples, it can be concluded that the barrier for internal rotation about the C—C bond must be larger than 12 kJ mol^{-1}. This lower limit also agrees fairly well with the gas-phase value, obtained from microwave spectroscopy (16.0 ± 6.0 kJ mol^{-1} [14]).

The experimental and 6-31G* calculated frequencies and intensities, as well as the PED for the *s-cis* and *s-trans* conformers, are shown in Tables 3 and 4. Table 5 presents the calculated values obtained for the higher energy *s-trans* (C—O) form. These tables also include the frequencies obtained with the scaled force fields. The latter show a

Table 3 Experimental and calculated vibrational wavenumbers and intensities for acrylic acid (*s-cis* form)[a]

approximate description	symmetry	exp (IR, Ar matrix)				calc (6-31G*)			
		ν	I	ν^{gc} [b]	I^{total} [c]	ν	I	ν^{scaled}	PED[d]
ν(O—H)	A′	3566.7	16.0	3564.8	30.4	4059	24.1	3557	s_1[100]
		3564.2	7.2						
		3561.3	7.2						
$\nu(CH_2)_{as}$	A′	no				3445	0.7	3021	s_2[98]
ν(C—H)	A′	no				3397	0.7	2980	s_3[94]
$\nu(CH_2)_s$	A′	no				3353	1.4	2941	s_4[96]
ν(C═O)	A′	1764.1	44.0	1762.4	80.0	2017	67.4	1777	s_5[91]
		1762.5	31.2						
		1746.0	4.8						
ν(C═C)	A′	1663.0	2.4	1638.8	15.2	1865	10.8	1645	s_6[73] + s_7[18] + s_9[10]
		1635.0	4.8						
		1633.9	8.0						
$\delta(CH_2)$	A′	1411.6	20.8	1410.8	47.2	1588	24.1	1403	s_7[61] + s_9[16] + s_{12}[11]
		1410.7	20.0						
		1408.2	6.4						
δ(C—O—H) + ν(C—O)	A′	1323.4	4.0	1323.4	4.0	1497	6.8	1324	s_8[20] + s_7[19] + s_{10}[18] + s_6[14] + s_{13}[10]
δ(C—H)	A′	1252.0		1252.0[e]		1417	0.2	1254	s_9[44] + s_8[20] + s_{11}[11]
ν(C—O) + δ(C—O—H)	A′	1194.0	5.6	1138.7	91.2	1319	76.5	1169	s_{10}[53] + s_8[40]
		1190.4	4.8						
		1132.2	51.2						
		1131.1	29.6						
$\omega(CH_2)$	A′	1060.7	4.8	1060.7	4.8	1176	3.0	1044	s_{11}[56] + s_9[24] + s_{12}[11]
ν(C—C)	A′	830.2	1.6	829.3	4.0	915	3.2	817	s_{12}[47] + s_{11}[19] + s_{10}[14]
		828.7	2.4						
δ(O═C—O)	A′	620.5	2.4	618.1	5.6	682	6.8	614	s_{13}[46] + s_{15}[16] + s_{16}[15] + s_{11}[10]
		616.3	3.2						
δ(C—C═O)	A′	491.8	3.6	491.8	3.6	533	4.2	484	s_{14}[30] + s_{13}[30] + s_{15}[13]
δ(C═C—C)	A′	no				298	0.5	279	s_{15}[58] + s_{14}[46]
$\Omega(CH_2)$	A″	994.0	5.2	990.6	10.0	1151	6.1	996	s_{16}[101]
		986.9	4.8						
Ω(C—H)	A″	973.4	3.6	972.5	6.8	1122	4.7	972	s_{17}[67] + s_{18}[36]
		971.4	3.2						
τ(C═C)	A″	812.4	8.8	812.4	8.8	921	14.8	806	s_{18}[32] + s_{20}[67] + s_{17}[10]
τ(C—O)	A″	610.1	19.2	609.8	21.6	690	21.1	614	s_{19}[71] + s_{18}[10]
		607.0	2.4						
Ω(C═O)	A″	448.8	4.4	488.8	4.4	529	4.7	481	s_{20}[40] + s_{19}[38] + s_{21}[19]
τ(C—C)	A″	no				122	0.3	143	s_{21}[76] + s_{17}[17] + s_{18}[10]

[a] Wavenumbers in cm^{-1}; ν, stretching; δ, bending; ω, wagging; Ω, out-of-plane; τ, torsion; no, not observed; s, symmetric; as, asymmetric. See Table 6 for coordinates definition. Experimental intensities presented are normalised values to the total intensity of the group of bands assigned to ν(C═O) in the *s-trans* conformer, which corresponds to the group of bands ascribed to a single vibration having the largest total intensity in the observed spectrum. Calculated intensities are normalised values to the calculated intensity of the band associated with the same vibration [ν(C═O) in *s-trans* form, whose non-normalised *ab initio* intensity is 526.9 km mol^{-1}]. The calculated intensities should be multiplied by 1.38 if a correction related with the relative population of the *s-cis* form to the *s-trans* form at room temperature, obtained from assuming a Boltzmann distribution and $\Delta E_{(s\text{-}trans)-(s\text{-}cis)} = 0.8$ kJ mol^{-1}, is considered. [b] ν^{gc} correspond to the wavenumbers of the gravity centres of the groups of bands ascribed to the same normal mode; they are calculated as $\nu^{gc} = \sum_i (\nu^{obs} \times I^{obs})/\sum_i I^{obs}$, where i is the number of total components of the group of bands. [c] I^{total} is the total intensity of the bands ascribed to the same normal mode. [d] PEDs < 10% are not presented in the table. [e] Value not used in the force field scaling.

general agreement with the experimental values to within 2% for the two experimentally observed conformers (see also Fig. 6).

All the conformers of acrylic acid belong to the C_s point group and thus their 21 normal modes span the irreducible representations, 15A′ + 6A″. Table 6 shows the C_s symmetry coordinates used in the normal coordinate analysis.

Most of the observed IR bands ascribable to individual conformers appear as close doublets resulting from molecules trapped in different matrix environments. Thus, for these cases, in order to make a more direct comparison with the calculated values, the gravity centres of the experimental bands were obtained [$\nu^{gc} = \sum_i(\nu^{obs} \times I^{obs})/\sum_i I^{obs}$; $I^t = \sum_i^{obs}$, with i being the number of components resulting from matrix site effects].

2800–3600 cm^{-1} *Region.* This spectral region includes the ν(O—H) and ν(CH) [$\nu(CH_2)_{as}$, $\nu(CH_2)_s$ and ν(C—H)] vibrations. The bands ascribable to the ν(CH) modes could not be observed experimentally in either Ar or Kr matrices. Indeed, in consonance with the experimental findings, the calculations predict that these modes should give rise to very low intensity IR bands in both the *s-cis* and *s-trans* conformers. In turn, their Raman activities were predicted to be rather large [the 6-31G* calculations predict that, together with the ν(O—H) and ν(C═C) modes, the ν(CH) vibrations are those giving rise to the most intense Raman bands], and in the Raman spectra of acrylic acid in diluted CCl_4 solutions, prominent bands appear at 2996, 3041 and 3110 cm^{-1}, which can be ascribed to the $\nu(CH_2)_{as}$, ν(C—H) and $\nu(CH_2)_s$, respectively (Fig. 7). The predicted (scaled) frequencies (see Tables 3 and 4) are somewhat lower than those observed in CCl_4 solution, but it is possible that, at least in part, this may result from solvent effects or be due to the involvement of the ν(CH) fundamentals in Fermi resonance interactions, as suggested by the appearance in the ν(CH) spectral region of a number of additional lower intensity bands.

The experimental and calculated frequencies and intensities associated with the ν(O—H) vibration agree very well. In particular, in agreement with the results of the calculations, the intensities of the IR bands originating in the two conformers

Table 4 Experimental and calculated vibrational wavenumbers and intensities for acrylic acid (*s-trans* form)[a]

approximate description	symmetry	exp. (IR, Ar matrix) ν	I	ν^{gc} [b]	I_{total} [c]	calc. (6-31G*) ν	I	ν^{scaled}	PED[d]
ν(O—H)	A′	3575.9	8.0	3572.8	26.8	4063	24.3	3560	s_1[100]
		3571.5	18.8						
$\nu(CH_2)_{as}$	A′	no				3445	0.9	3021	s_2[97]
ν(C—H)	A′	no				3400	0.5	2982	s_3[95]
$\nu(CH_2)_s$	A′	no				3355	1.4	2943	s_4[95]
ν(C=O)	A′	1759.9	24.0	1757.6	100.0	2029	100.0	1788	s_5[87]
		1757.4	52.0						
		1755.9	24.0						
ν(C=C)	A′	1651.4	2.0	1631.0	9.2	1853	1.9	1634	s_6[72] + s_7[21]
		1625.7	5.6						
		1623.8	1.6						
$\delta(CH_2)$	A′	1416.0	9.6	1416.0	9.6	1587	8.7	1403	s_7[62] + s_{12}[12]
ν(C—O) + δ(C—O—H)	A′	1329.7	8.8	1329.7	8.8	1510	16.1	1335	s_{10}[28] + s_8[18] + s_{13}[15] + s_7[14] + s_{12}[11]
δ(C—H)	A′	no				1428	0.6	1264	s_9[55] + s_{11}[15] + s_6[12]
δC—O—H) + ν(C—O)	A′	1187.0	6.4	1185.0	36.8	1352	39.5	1198	s_8[63] + s_{10}[24]
		1184.6	30.4						
$\omega(CH_2)$	A′	1019.2	18.4	1018.3	30.0	1140	11.4	1013	s_{11}[54] + s_{10}[23] + s_9[20]
		1016.9	11.6						
ν(C—C)	A′	825.9	2.0	825.9	2.0	912	2.3	814	s_{12}[44] + s_{10}[21] + s_{11}[14]
δ(O=C—O)	A′	580.5	7.2	580.5	7.2	638	10.0	576	s_{13}[65] + s_{15}[20] + s_8[11]
δ(C—C=O)	A′	525.0	0.8	525.0	0.8	578	1.9	523	s_{14}[40] + s_{15}[16] + s_{12}[14] + s_{13}[13]
δ(C=C—C)	A′	no				305	0.3	285	s_{15}[53] + s_{14}[45]
$\Omega(CH_2)$	A″	998.6	4.0	996.1	6.0	1114	4.9	990	s_{16}[99]
		991.2	2.0						
Ω(C—H)	A″	970.6	5.2	968.7	14.4	1130	7.0	979	s_{17}[61] + s_{18}[29] + s_{21}[10]
		968.1	5.2						
		967.1	4.0						
τ(C=C)	A″	816.2	17.6	816.2	17.6	919	13.7	804	s_{18}[27] + s_{20}[65] + s_{21}[10]
τ(C—O)	A″	568.4	14.4	567.5	44.0	645	21.8	577	s_{19}[75] + s_{18}[10]
		567.0	29.6						
Ω(C=O)	A″	475.9	4.0	474.0	8.0	526	0.4	478	s_{20}[44] + s_{19}[32] + s_{17}[26]
		472.0	4.0						
τ(C—C)	A″	no				122	0.0	143	s_{21}[89] + s_{18}[19]

[a] See Table 3 for definitions. See Table 6 for coordinates definition. Experimental intensities presented are normalised values to the total intensity of the group of bands assigned to ν(C=O), which corresponds to the group of bands ascribed to a single vibration having the largest total intensity in the observed spectrum. Calculated intensities are normalised values to the calculated intensity of the band associated with the same vibration [ν(C=O)], whose non-normalised *ab initio* intensity is 526.9 km mol^{-1}. [b] ν^{gc} correspond to the wavenumbers of the gravity centers of the groups of bands ascribed to the same normal mode; they are calculated as $\nu^{gc} = \sum_i(\nu^{obs} \times I^{obs})/\sum_i I^{obs}$, where i is the number of total components of the group of bands. [c] I^{total} is the total intensity of the bands ascribed to the same normal mode. [d] PEDs < 10% are not presented in the table.

Table 5 Calculated vibrational wavenumbers and intensities for acrylic acid [*s-trans* (C—O) form][a]

approximate description	symmetry	calc. (6-31G*) ν	I	ν^{scaled}	PED[b]
ν(O—H)	A′	4120	16.0	3610	s_1[100]
$\nu(CH_2)_{as}$	A′	3448	0.4	3024	s_2[99]
$\nu(CH_2)_s$	A′	3361	2.4	2948	s_4[77] + s_3[23]
ν(C—H)	A′	3341	1.8	2931	s_3[77] + s_4[23]
ν(C=O)	A′	2049	61.4	1804	s_5[92]
ν(C=C)	A′	1860	11.3	1640	s_6[74] + s_7[18] + s_9[11]
$\delta(CH_2)$	A′	1580	25.1	1344	s_7[67] + s_9[20]
ν(C—O) + δ(C—O—H)	A′	1472	36.0	1302	s_{10}[22] + s_6[17] + s_9[16] + s_7[15] + s_8[14]
δ(C—H)	A′	1447	69.6	1280	s_9[28] + s_8[41] + s_{10}[15]
δ(C—O—H) + ν(C—O)	A′	1283	4.5	1138	s_8[32] + S_{10}[39]
$\omega(CH_2)$	A′	1173	0.2	1042	s_{11}[51] + s_9[23] + s_{12}[13]
ν(C—C)	A′	927	2.3	827	s_{12}[44] + s_{11}[18] + s_{10}[17] + s_{13}[13]
δ(O=C—O)	A′	694	2.1	624	s_{13}[45] + s_{15}[16] + s_{14}[18] + s_{11}[12]
δ(C—C=O)	A′	542	0.1	492	s_{14}[30] + s_{13}[26] + s_{15}[10] + s_{12}[10]
δ(C=C—C)	A′	310	1.8	290	s_{15}[61] + s_{14}[40]
$\Omega(CH_2)$	A″	1156	6.3	1000	s_{16}[101]
Ω(C—H)	A″	1101	4.7	955	s_{17}[70] + s_{18}[36]
τ(C=C)	A″	903	10.2	791	s_{18}[29] + s_{20}[68]
Ω(C=O)	A″	542	2.8	517	s_{20}[28] + s_{18}[32] + s_{17}[20] + s_{21}[11]
τ(C—O)	A″	450	24.6	415	s_{19}[76] + s_{20}[16] + s_{17}[11]
τ(C—C)	A″	99	0.2	124	s_{21}[92]

[a] See Table 3 for definitions. See Table 6 for coordinates definition. Calculated intensities are normalised values to the calculated intensity of the band associated with ν(C=O) in the *s-trans* conformer. [b] PEDs < 10% are not presented in the table.

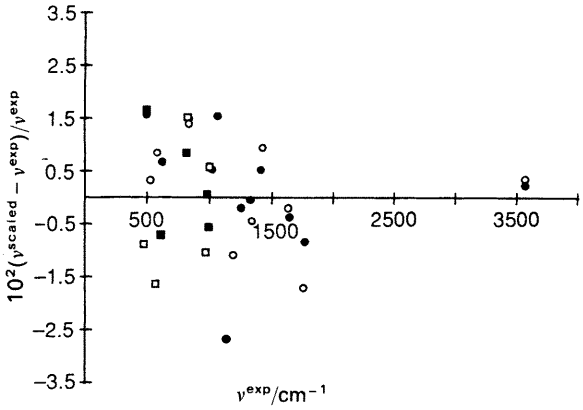

Fig. 6 Differences between the SCF-HF/6-31G* calculated (scaled) wavenumbers and the experimental values [$100 \times (\nu^{scaled} - \nu^{exp})/\nu^{exp}$%]. ●, In-plane *s-cis*; ○, in-plane *s-trans*; ■, out-of-plane *s-cis*; □, out-of-plane *s-trans*. The scaled values were calculated from the optimised straight lines obtained by fitting calculated to experimental wavenumbers using two different linear regressions, one for in-plane vibrations, and the other for out-of-plane modes (see text). The straight lines obey the equations: ν^{scaled} (in-plane) $= 0.871 \times \nu^{ab\ initio} + 19.713$ ($R^2 = 0.9993$); ν^{scaled} (out-of-plane) $= 0.829 \times \nu^{ab\ initio} + 42.287$ ($R^2 = 0.9987$).

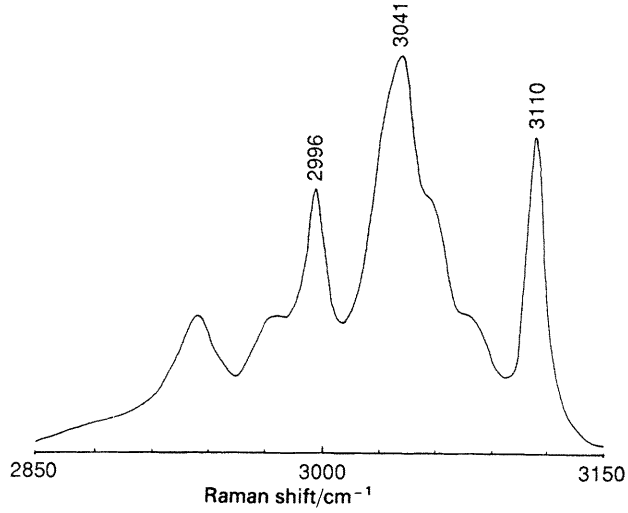

Fig. 7 ν(CH) stretching region of the Raman spectrum of acrylic acid in diluted CCl_4 solution (room temperature)

were found to be similar and the frequency of the *s-cis* vibration was found to be slightly lower than that corresponding to the *s-trans* form. The calculations also predict that the ν(O—H) stretching mode in the *s-trans* (C—O) conformer is larger than in both *s-cis* and *s-trans* forms (see Tables 3–5). This result can be correlated with the absence in the *s-trans* (C—O) form of the above mentioned C=O···O—H through-space field interaction that polarises the O—H bond in the most stable *s-cis* (C—O) conformers (*s-cis* and *s-trans*) leading to reduced k_{OH} force constants and, consequently, to lower ν(O—H) vibrational frequencies.

Note that the predicted intensity of the ν(O—H) IR band of the *s-trans* (C—O) conformer is considerably lower than in the two observed conformers. In general, the intensity of a well localised ν(X—Y) stretching vibration (in particular when Y is a hydrogen atom) can be properly described[55] by

$$I^{\nu X-Y} \propto \{\zeta^{\circ}_{corr}(Y) + [\partial\zeta_{corr}(Y)/\partial R_{X-Y}]R^{\circ}_{X-Y}\}^2$$

where ζ°_{corr} and $(\zeta_{corr}/R_{X-Y})R^{\circ}_{XY}$ (abbreviated X—Y →) are the equilibrium Mulliken corrected charges on the atom Y and the charge-flux associated with the stretching of the R_{X-Y} bond from its equilibrium position, R°_{X-Y}, respectively. Since the corrected Mulliken charges on the carboxylic hydrogen atom are very similar in the three conformers (*ca.* 0.39 *e*; see Fig. 4), it can be concluded that it is the charge-flux term that must be considerably smaller in the *s-trans* (C—O) form than in the two observed conformers. Indeed, the charge-flux reduces from *ca.* -0.80 *e* Å^{-1}, in both *s-cis* and *s-trans* forms, to about -0.72 *e* Å^{-1}, in the *s-trans* (C—O) form.

In the case of the ν(CH) stretching modes, their average low intensity correlates very well with the corresponding average corrected Mulliken charges on hydrogens and

Table 6 Definition of the internal symmetry coordinates used in the normal-coordinate analysis[a]

coordinate	approximate description	symmetry	definition
S_1	ν(O—H)	A′	ν(O—H)
S_2	$\nu(CH_2)_{as}$	A′	ν(C—H) − ν(C—H′)
S_3	ν(C—H)	A′	$\nu(C_\alpha—H)$
S_4	$\nu(CH_2)_s$	A′	ν(C—H) + ν(C—H′)
S_5	ν(C=O)	A′	ν(C=O)
S_6	ν(C=C)	A′	ν(C=C)
S_7	$\delta(CH_2)$	A′	2δ(H—C—H′) − δ(H—C=C) − δ(H′—C=C)
S_8	δ(C—O—H)	A′	δ(C—O—H)
S_9	δ(C—H)	A′	δ(C—C—H) − δ(C=C—H)
S_{10}	ν(C—O)	A′	ν(C—O)
S_{11}	$\omega(CH_2)$	A′	δ(H—C=C) − δ(H′—C=C)
S_{12}	ν(C—C)	A′	ν(C—C)
S_{13}	δ(O=C—O)	A′	2δ(O=C—O) − δ(C—C=O) − δ(C—C—O)
S_{14}	δ(C—C=O)	A′	δ(C—C=O) − δ(C—C—O)
S_{15}	δ(C=C—C)	A′	2δ(C=C—C) − δ(C—C—H) − δ(C=C—H)
S_{16}	$\Omega(CH_2)$	A″	Ω[H—C(=C)—H′]
S_{17}	Ω(C—H)	A″	Ω[C=C(—H)—C]
S_{18}	τ(C=C)	A″	τ(H—C=C—C) + τ(H′—C=C—C) + τ(H—C=C—H) + τ(H′—C=C—H)
S_{19}	τ(C—O)	A″	τ(H—O—C=O) + τ(H—O—C—C)
S_{20}	Ω(C=O)	A″	Ω[C—C(=O)—O]
S_{21}	τ(C—C)	A″	τ(H—C—C=O) + τ(H—C—C—O) + τ(C=C—C=O) + τ(C=C—C—O)

[a] Normalization constants are not given here; they are chosen as $N = (\sum c_i^2)^{-1/2}$, where c_i are the coefficients of the individual valence coordinates; see Table 3 for definitions.

C—H → charge-fluxes (*ca.* 0.15 *e* and −0.21 *e* Å^{-1}, respectively). These relatively low values of ζ°_{corr}(H) and C—H → now obtained for acrylic acid are, in fact, typical values of ethenic hydrogens,[49–51,55] although they are considerably different from the corresponding values found, for instance, in formaldehyde,[52] where the back-donation effect from the *trans* lone electron pair of the carbonyl oxygen to the σ^* antibonding orbital of the C—H bond causes, besides a large increase in the C—H bond length, a reduction in ζ°_{corr}(H) to *ca.* 0.064 *e* and an increase in the C—H → charge-flux term to −0.30 *e* Å^{-1}, leading to a strong increase of the ν(CH) IR bands.[52,56]

850–1800 cm^{-1} *Region.* This spectral region includes the ν(C=C) and ν(CO) [both ν(C=O) and ν(C—O)] stretching modes, the δ(CH) bending vibrations [in plane: $\delta(CH_2)$, δ(C—H), $\omega(CH_2)$; out-of-plane: $\Omega(CH_2)$, Ω(C—H)] and the δ(C—O—H) in-plane bending mode. In this spectral region, the agreement between calculated and experimental data is very good in both frequency and intensity (see Tables 3 and 4 and Fig. 5 and 6).

In the case of the *s-cis* conformer, the three intense groups of IR bands with gravity centres at 1762, 1410 and 1139 cm^{-1} dominate the spectrum. These bands are easily assigned to the ν(C=O), $\delta(CH_2)$ and ν(C—O) + δ(C—O—H) vibrations, which are predicted by the calculations to have very large IR intensities. Note that the ν(C—O) and δ(C—O—H) coordinates were found to be considerably mixed and thus, it appears to be more correct to assign the band at 1139 cm^{-1} as well as the band appearing at 1323 cm^{-1} to 'hybrid' vibrations having significant contributions from these two coordinates, than trying to assign each one of these bands to just a single coordinate. By comparing the calculated and experimental data, the assignments of the remaining bands are also not very difficult (see Table 3). The following additional conclusions shall, however, be stressed:

(i) The δ(C—H) mode is predicted to give rise to a very low intensity band at *ca.* 1254 cm^{-1}. Thus, the band due to this vibration probably contributes to the total intensity of the IR band observed at 1252 cm^{-1}, which also contains an important contribution from dimer structures;

(ii) The presence of the lower component of the group of bands ascribed to ν(C=O) with a frequency (1746 cm^{-1}) considerably lower than those of the other two components (1764 and 1761 cm^{-1}) seems to indicate that the ν(C=O) mode originating in one set of molecules occupying a particular site within the matrix is involved in a Fermi resonance interaction [probably with the τ(C=C) + Ω(C—H) combination band, whose associated fundamentals have gravity centres at 812 and 972 cm^{-1}, respectively; see Table 3]. Considering the relative intensities of the three ν(C=O) bands (1746 cm^{-1}: 4.8; 1761 cm^{-1}: 31.2; 1764 cm^{-1}: 44.0), and assuming both identical populations of molecules and similar intensity perturbations due to interactions with the matrix in the two different observed matrix sites, the Fermi doublet can be easily identified as corresponding to the 1746 and 1761 cm^{-1} pair of bands.

(iii) Similar Fermi resonance interactions involving the ν(C=C) and ν(CO) + δ(C—O—H) vibrations seem also to occur. Indeed, these kinds of interactions, mainly involving ν(C=O) or ν(C=C), have often been observed in α-substituted carbonyls, even when matrix-isolated data are considered.[40–42,57] In the case of ν(C=C), the pair of bands appearing at 1663 and 1635 cm^{-1} are most probably a Fermi resonance doublet originated in one particular set of molecules in a given matrix site [this Fermi interaction involves possibly the first overtone of the ν(C—C) mode, whose fundamental has a gravity centre at 829 cm^{-1}], while the 1634 cm^{-1} band originates in a second set of molecules in a different site. In the case of the ν(CO) + δ(C—O—H) vibration, four bands appear in the spectrum, indicating that all molecules have their ν(CO) + δ(C—O—H) fundamental involved in Fermi resonance, most probably with the first overtone of the τ(C—O) vibration, whose fundamental has a gravity centre at 610 cm^{-1}. However, in this case the unambiguous identification of the two Fermi doublets could not be undertaken, since it is apparent that the interactions with the matrix, in the two matrix sites observed, affect the intensities of this vibration in different ways.

The IR spectrum of the *s-trans* conformer in this spectral region has essentially a general profile similar to that of the *s-cis* form (see Fig. 5 and Tables 3 and 4).

(i) Also in this case the spectrum is dominated by three intense groups of bands having gravity centres at 1758, 1185 and 1018 cm^{-1}, which are ascribable to ν(C=O), δ(C—O—H) + ν(C—O) and $\delta(CH_2)$, respectively.

(ii) The ν(C—O) and δ(C—O—H) coordinates are also considerably mixed in this form. However, the contribution of the δ(C—O—H) coordinate to the band at *ca.* 1185 cm^{-1} is now relatively more important than in the case of the *s-cis* conformer, while its contribution to the band at *ca.* 1325 cm^{-1} is relatively less important.

(iii) Finally, Fermi resonance interactions similar to those found in the case of the *s-cis* form, involving the ν(C=O), ν(C=C) and ν(C—O) + δ(C—O—H), are also observed in the *s-trans* form for ν(C=O) and ν(C=C). The doublets of Fermi origin in one set of molecules in a particular site corresponding to ν(C=O) and ν(C=C) are the 1760/1756 cm^{-1} and 1651/1624 cm^{-1} pairs of bands, respectively, while in each case a third band is also observed, corresponding to the ν(C=O) (1757 cm^{-1}) or ν(C=C) (1651 cm^{-1}) vibration of a second set of molecules in a different site, not involved in Fermi resonance interactions.

Comparing now the frequencies of the two conformers, note that in the case of ν(C=O) only, the relative order of calculated (scaled) frequencies does not agree with the experimental data [*i.e.* the ν(C=O) frequency of the *s-cis* form is calculated as being lower than that of the *s-trans* form, while the opposite situation was observed experimentally]. Though the possibility of this inversion in the relative order of ν(C=O) being essentially related to an intrinsic deficiency of the basis set used in the calculations cannot be ruled out, it is possible that, at least in part, this inversion results from the existence in the two forms of different interactions between the carbonyl bond and the matrix. Indeed, it is well known that the frequency of the ν(C=O) vibration is extremely sensitive to the molecular environment, in particular when the C=O bond is exposed to the bulk particles. For example, red shifts of 5–15 cm^{-1} in ν(C=O) have been observed upon changing the polarity of the solvent for several carbonyl molecules in dilute solutions of aprotic solvents,[58] and even larger red shifts (*ca.* 30 cm^{-1}) are often found upon going from the vapour phase to solutions of apolar solvents such as CCl_4.[39,40] If such a matrix–substrate interaction is, in fact, operating in the studied system, the *s-trans* conformer will be the one which will suffer the largest red shift, since the C=O bond in this form is considerably more accessible than in the *s-cis* conformer, and this may lead to an inversion in the relative order of frequencies of the ν(C=O) mode in the two conformers. A detailed study of the temperature dependence of the vapour-phase spectrum of acrylic acid must, however, be undertaken in order to verify this possibility.

Comparing the calculated ν(C=O) frequencies of the two experimentally observed conformers with that predicted for the higher-energy *s-trans* (C—O) form, it can be seen that in the latter this frequency is substantially higher (see Tables 3, 4 and 6). As in the case of ν(O—H), this relative order of

frequencies can also be understood considering the effects of the presence or not in the various conformers of the C=O···O—H through-space field interaction. Indeed, in the two experimentally observed forms (which have the O=C—O—H axis in the *s-cis* conformation and thus have the dipoles associated with their C=O and O—H bonds nearly antiparallel) the presence of the C=O···O—H through-space field interaction increases the polarisation of the C=O bond and leads to a reduction in the ν(C=O) frequency.

On the other hand, the ν(C=O) IR intensities appear to be related to the relative orientation of the two double bonds (*i.e.* the conformation of the C=C—C=O axis). Thus, the two conformers having the C=C—C=O axis in the *s-cis* conformation [the most stable *s-cis* form and the *s-trans* (C—O) form] have a ν(C=O) intensity that is about 1.5 times less intense than that of the *s-trans* conformer. Since the charges of the carbonyl oxygen atom are very similar in the three conformers (*ca.* −0.48 *e*; Table 7), it can be concluded that in this case also, the charge-flux term has a dominant contribution to the observed ν(C=O) intensity differences between the two different orientations of the C=C—C=O axis. In fact, the calculated C=O→ charge-flux is *ca.* −0.83 *e* Å^{-1} in both conformers having an *s-cis* C=C—C=O axis while it increases to *ca.* −1.02 *e* Å^{-1} in the *s-trans* form. Note that both the charge and charge-flux terms in the two conformers with an *s-cis* C=C—C=O axis are similar to those previously found for HC(=O)OH[52] [note that the *s-cis* (C—O) and *s-trans* (C—O) conformers of HC(=O)OH have very similar charges on the carbonyl oxygen and C=O→ charge-fluxes; see Table 7]. This result points to a reduced interaction between the two double bonds in these conformers. On the other hand, the charge-flux term in the *s-trans* conformer is closer to this term in HC(=O)SH,[52] despite the fact that the charge on the carbonyl oxygen atom is considerably smaller in this latter molecule [which thus has a lower ν(C=O) intensity than the *s-trans* form of acrylic acid]. Hence, it can be concluded that the electronic interaction between the C=C and C=O bonds is more important in the *s-trans* form than in the remaining conformers, a result which is in agreement with the conclusions presented in the previous section taken on the basis of relative values of the geometrical parameters in the various conformers. This conclusion is also reinforced by the fact that the IR intensities of the bands due to ν(C=C) in the different conformers can also be successfully correlated with the proposed relative extent of mesomerism involving the C=C and C=O bonds in each form, the lower the importance of this mesomerism [*s-trans* > *s-cis* ≈ *s-trans* (C—O)], the more intense is the ν(C=C) IR band.

Finally, it is also important to note that the predicted Ω(C—H) and Ω(CH_2) average normalised intensities per C—H bond, calculated using the CCFO model, agree very well with the observed average normalised intensities. For planar molecules, the charge-flux term related with out-of-plane vibrations is zero and thus, only the term related with the charge on the H atoms (average value *ca.* 0.15 *e*, in all forms) contributes to the total intensity of the two Ω(CH) modes. The calculated value (average normalised intensity per C—H bond) obtained using the CCFO model is 4.1, which compares very well with the corresponding experimental [*s-cis*, 5.6; *s-trans*, 6.8) or *ab initio* calculated [*s-trans* (C—O), 3.7] values.

400–850 cm^{-1} *Region.* In this spectral region appear the bands due to the ν(C—C) stretching mode, the δ(O=C—O), δ(C—C=O) and Ω(C=O) bending vibrations and both the τ(C=C) and τ(C—O) torsions. As for the other spectral regions, the results of the theoretical calculations and the experimental data agree quite well as regards the frequencies and relative intensities of the bands ascribable to these vibrations in the experimentally observed conformers (see Tables 3 and 4). The assignment of the τ(C—O) mode to the IR bands at 610 cm^{-1} (*s-cis*) and 586 cm^{-1} (*s-trans*) is particularly clear, owing to its predicted high intensity (see Fig. 5 and Tables 3 and 4).

Region below 400 cm^{-1}. In this spectral region the δ(C=C—C) bending vibration and the τ(C—C) torsional mode were expected to occur. This spectral region was not covered by our IR studies and the Raman data obtained for the dilute solution of acrylic acid in CCl_4 did not help very much, since the very strong features due to the solvent appearing in this spectral region precluded the detection of any band due to the solute. However, a medium intensity broad band could be observed at *ca.* 300 cm^{-1} in the Raman spectrum of acrylic acid dissolved in acetonitrile, which probably contains contributions of the δ(C=C—C) mode in both conformers (calculated frequencies are 298 and 285 cm^{-1}, respectively, for the *s-cis* and *s-trans* conformer). In turn, the calculated frequencies of the τ(C—C) mode (143 cm^{-1} in both forms) are considerably overestimated when compared with the gas-phase values obtained by microwave spectroscopy (*s-cis*: 105 cm^{-1}; *s-trans*: 95 cm^{-1} [14]), a result which is certainly related to the overestimation by the calculations of the energy barrier for internal rotation about the C—C bond.

Vibrational Data for Condensed Phases

The IR and Raman room-temperature spectra of liquid acrylic acid and the Raman spectrum of this compound in the crystalline phase at *ca.* −10 °C are shown in Fig. 8. Table 8 presents the corresponding vibrational assignments, which

Table 7 Equilibrium corrected Mulliken charges on the carbonyl oxygen atom [ζ°_{corr}(O)] and C=O→ charge fluxes {[$\partial\zeta_{corr}$(O)/$\partial R_{C=O}$]$R^{\circ}_{C=O}$} associated with the carbonyl stretching[a]

molecule		$-[\partial\mu_{C=O}/\partial R_{C=O}]_{(O)}$[b]	$-\zeta^{\circ}_{corr}$(O)	$-[\partial\zeta_{corr}(O)/\partial R_{C=O}]R^{\circ}_{C=O}$	ref.
acrylic acid	*s-cis*	1.318	0.489	0.829	this work
	s-trans	1.511	0.493	1.018	
	s-trans(C-O)	1.317	0.488	0.829	
H_2C=O		1.072	0.406	0.666	50
HC(=O)OH	*s-cis*(C—O)	1.326	0.479	0.847	50
	s-trans(C—O)	1.355	0.468	0.887	
HC(=O)SH	*s-cis*(C—S)	1.426	0.364	1.062	50
	s-trans(C—S)	1.436	0.381	1.055	

[a] Charges in *e*; charge-fluxes in *e* Å^{-1}. [b] $[\partial\mu_{C=O}/\partial R_{C=O}]_{(O)} = \zeta^{\circ}_{corr}(O) + [\partial\zeta_{corr}(O)/\partial R_{C=O}]R^{\circ}_{C=O}$ is the polar tensor element of the oxygen atom which is directly associated with the C=O→ stretching intensity[52,55] (see text), and corresponds to the partial derivative of the component of the molecular dipole moment along the C=O direction with respect to the displacement of the oxygen atom during the C=O stretching vibration, assuming the carbon atom is fixed at the origin of the reference.

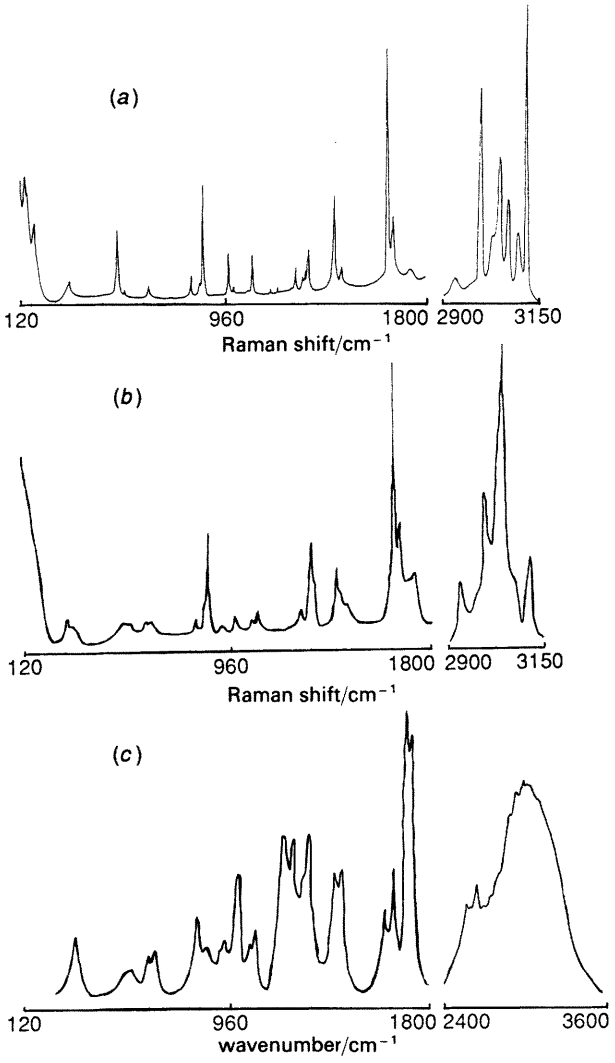

Fig. 8 Vibrational spectra of acrylic acid in (*a*) crystalline (Raman, $T = -10\,°C$), (*b*) liquid (Raman, room temperature) and (*c*) (IR, room temperature) phases

are fully consistent with the data obtained for the monomer discussed above and greatly improve on the assignments previously reported.[7,9]

The structure of crystalline acrylic acid has been determined by X-ray diffraction[8] and it was found that this compound crystallises in planar hydrogen-bonded dimers across a symmetry centre. The measured value of 95 pm for the O—H distance in the crystal, however, leaves no doubt that the hydrogen atom is singly bonded and not symmetrical in the hydrogen bond.[8] In addition, the crystallographic studies also indicated that individual molecules adopt an *s-cis* structure both about the C=C—C=O and O=C—O—H axes.[8]

The dimeric molecule possesses global C_{2h} symmetry but, since the coupling between monomer units is by hydrogen bonds rather than by the stronger (normal) chemical bonds, it may be anticipated that the vibrational selection rules cannot hold rigorously. In fact, the results indicate that the coupling between the two monomer units is not sufficiently great to cause observable frequency differences in the same vibration of each monomer unit, except in the case of the two bending modes involving the carboxylic hydrogens [in-plane, δ(C—O—H), and out-of-plane, τ(C—O)], which are directly involved in the hydrogen bond. In these two cases, bands due to the in-phase and out-of-phase vibrations of the coupled oscillators can be observed (see Fig. 8 and Table 8).

In agreement with the crystallographic data, in the crystalline phase Raman spectrum only bands ascribable to monomer units in the *s-cis* conformation can be observed, displaying the rather large difference of the hydrogen bond strength between *s-cis/s-cis* and *s-trans/s-trans* dimers. In turn, in the liquid-phase spectra (both Raman and IR) additional bands appear, which can be ascribed to monomer units in the *s-trans* conformation. Indeed, the relative frequencies of these new bands and those bands assigned to the same vibration in the crystal follow the same pattern observed for the *s-trans vs. s-cis* relative frequencies in the Ar-matrix spectra.

From the analysis of the spectra obtained for acrylic acid in the condensed phases, the following conclusions can also be drawn:

(i) ν(CH) modes [$\nu(CH_2)_{as}$, ν(C—H) and $\nu(CH_2)_s$] are easily ascribed to the Raman bands at 3108, 3041 and 2996 cm^{-1}, respectively, in the spectrum of the crystal (in the Raman spectrum of the liquid these bands appear at very similar wavenumbers; 3110, 3040 and 2996 cm^{-1}). In the IR spectrum of the liquid, the corresponding bands are obscured by the strong, very broad group of bands due to ν(O—H);

(ii) In the *s-cis* monomer units, the $\nu(CO_2)_{as}$ and $\nu(CO_2)_s$ stretching vibrations give rise to the very intense IR bands at 1725 and 1432 cm^{-1}, respectively, which have counterparts in the low intensity Raman bands appearing at 1721 and 1444 cm^{-1} (solid-state spectrum) or 1725 and 1430 cm^{-1} (liquid). The corresponding bands belonging to *s-trans* monomeric units appear at 1705 and 1418 cm^{-1} (IR) or 1705 and 1408 cm^{-1} (Raman); these are absent in the crystalline-phase spectrum.

(iii) In the Raman spectrum of the crystal, ν(C=C) appears as a Fermi resonance doublet (1657 and 1637 cm^{-1}). In the liquid-phase Raman spectrum, in addition to this Fermi doublet, a new band at 1620 cm^{-1} appears, which is ascribable to the ν(C=C) vibration of the *s-trans* monomeric units (not involved in Fermi resonance).

(iv) As referred to above, both the in-plane and out-of-plane bending vibrations involving the carboxylic hydrogen atoms [δ(C—O—H) and τ(C—O), respectively], owing to the coupling between the two monomeric units of the dimers, are split in in-phase and out-of-phase vibrations. As expected, the two out-of-phase vibrations give rise to intense IR bands [δ(C—O—H) out-of-phase: 1291 cm^{-1}; τ(C—O) out-of-phase: 1186 cm^{-1}], which have very low intensities in the Raman spectra [in the Raman spectrum of the crystal, δ(C—O—H) out-of-phase corresponds to a Fermi resonance doublet of slightly higher total intensity than in the liquid-phase Raman spectrum]. In turn, the in-phase δ(C—O—H) vibration (1280 cm^{-1}, liquid; 1292/1283 cm^{-1}, Fermi doublet, crystal) is very intense in the Raman spectra, and has a relatively low intensity in the IR spectrum. On the other hand, the τ(C—O) in-phase vibration only appears as a very low intensity band in the Raman spectrum of the crystal (1149 cm^{-1}), being absent both in the Raman and IR spectra of the liquid.

Finally, note that, while in general the frequencies corresponding to the matrix-isolated spectra (monomers) and condensed phases (dimers) do not differ very much, there are important exceptions, all of them easily correlated with the structural changes due to the hydrogen bond formation. Thus, the greater similarity of the two CO bonds in the dimers leads to the usual order of frequencies,

$$\underset{\text{(monomer)}}{\nu(=O)} > \underset{\text{(dimer)}}{\nu(CO_2)_{as}} > \underset{\text{(dimer)}}{\nu(CO_2)_s} > \underset{\text{(monomer)}}{\nu(C-O)}$$

The two bending vibrations involving the carboxylic hydrogen atoms [δ(C—O—H) and τ(C—O)] are strongly blue-shifted upon dimer formation, since the movements of these

Table 8 Experimental vibrational wavenumbers and relative intensities for acrylic acid in the crystalline (−10 °C) and pure liquid (room temperature) phases[a]

approximate description	crystal (Raman) *s-cis*	liquid (Raman) *s-cis*	liquid (Raman) *s-trans*	liquid (IR) *s-cis*	liquid (IR) *s-trans*
ν(OH)				3200–2500 vs, vb	
$\nu(CH_2)_{as}$	3108 m		3110 m		
ν(C—H)	3041 w		3040 s		
$\nu(CH_2)_s$	2996 m		2996 w		
$\nu(CO_2)_{as}$	1721 w	1725 m,	1705 m	1725 s,	1705 vs
ν(C=C)	1657 s	1658 s,	1620 s, sh	1638 s,	1620 s
	1637 vs		1636 vs		
$\nu(CO_2)_s$	1444 m	1430 m,	1408 m, sh	1432 s,	1418 m
$\delta(CH_2)$	1414 s		1396 s	1384 m	
δ(C—O—H) (out-of-phase)	1305 m		1295 m, sh	1291 s	
	1301 m				
δ(C—O—H) (in-phase)	1292 m		1280 s	1281 m	
	1283 m				
δ(C—H)	1252 m		1236 m	1244 s	
τ(C—O) (out-of-phase)	1182 vw			1186 s	
τ(C—O) (in-phase)	1149 vw				
$\omega(CH_2)$	1073 m	1068 m,	1044 m	1063 m,	1048 m
$\Omega(CH_2)$	993 w		993 w, sh	990m	
Ω(C—H)	973 m	997 m,	926 w	976 m, sh,	925 m
ν(C—C)	867 s		861 s	860 m	
τ(C=C)	818 m		818 m	818 m	
δ(O=C—O)	642 m	642 m,	628 m	650 m,	630 m
$\omega(CO_2)$	535 w	525 w,	548 w	525 w,	552 w
$\Omega(CO_2)$	516 s		517 m	512 vw	
δ(C=C—C)	318 m	306 m,	337 m	302 w,	336 m
τ(C—C)	139 (?) s			(155)[b]	

[a] See Table 3 for definitions; vs, very strong; s, strong; m, medium; w, weak; vw, very weak; sh, shoulder; vb, very broad. [b] In cyclohexane solution.[7]

atoms in the dimers are considerably restricted by the existence of the hydrogen bond. Finally, the frequencies of the δ(C—C=O) and Ω(C=O) modes of the monomers are somewhat different from those of their corresponding vibrations in the dimers, better described as $\omega(CO_2)$ and $\Omega(CO_2)$, owing to the similarity of the two oxygen atoms in the dimer.

R.F. acknowledges the financial support from Junta Nacional de Investigação Científica e Tecnológica, JNICT, Lisboa. J.N. would like to thank the Academy of Finland and NorFA for financial support.

References

1 V. Vijayalakshmi, J. N. R. Vani and N. Krishnamurti, *Eur. Polym. Paint Colour J.*, 1991, **181**, 506.
2 K. Katada, H. Sano, Y. Katoh, V. K. Jain, S. Mashita, A. Takenchi and S. Koga, *Acta Radiol. Suppl. Stockh.*, 1986, **369**, 623.
3 A. N. Brito, N. Correia, S. Svensson and H. Agren, *J. Chem. Phys.*, 1991, **95**, 2965.
4 P. R. Carey, *Biochemical Applications of Raman and Resonance Raman Spectroscopies*, Academic Press, London, 1982.
5 P. J. Tonge and P. R. Carey, *Biochemistry*, 1990, **29**, 10723.
6 R. Fausto, *Ciên. Biol.*, 1988, **13**, 1.
7 W. R. Feairheller Jr. and J. E. Katon, *Spectrochim. Acta, Part A*, 1967, **23**, 2225.
8 M. A. Higgs and R. L. Sass, *Acta Crystallogr.*, 1963, **16**, 657.
9 P. F. Krause, J. E. Katon and K. K. Smith, *Spectrochim. Acta, Part A*, 1975, **32**, 957.
10 J. R. Cowles, W. O. George and W. G. Fateley, *J. Chem. Soc., Perkin Trans. 2*, 1975, 396.
11 K. Bolton, N. L. Owen and J. Sheridan, *Nature (London)*, 1968, **218**, 226.
12 J. Umamura and S. Hayashi, *Bull. Inst. Chem. Res., Kyoto Univ.*, 1974, **52**, 85.
13 T. Ukaji, *Bull. Chem. Soc. Jpn.*, 1959, **32**, 1266.
14 K. Bolton, D. G. Lister and J. Sheridan, *J. Chem. Soc., Faraday Trans. 2*, 1974, **70**, 113.
15 A. I. Kiss and I. Lukovitz, *Chem. Phys. Lett.*, 1979, **65**, 169.
16 R. J. Loncharich, T. R. Schwartz and K. N. Honk, *J. Am. Chem. Soc.*, 1987, **109**, 14.
17 S. W. Charles, F. C. Cullen, N. L. Owen and G. A. Williams, *J. Mol. Struct.*, 1987, **157**, 17.
18 K. Fan and J. E. Boggs, *J. Mol. Struct.*, 1987, **157**, 31.
19 P. Pulay, G. Fogarasi, G. Pongor, J. E. Boggs and A. Vargha, *J. Am. Chem. Soc.*, 1983, **105**, 7037.
20 K. B. Wiedberg and K. E. Laidig, *J. Am. Chem. Soc.*, 1987, **109**, 5935.
21 S. E. Galembeck and R. Fausto, *J. Mol. Struct. (Theochem.)*, in the press.
22 W. T. King and G. B. Mast, *J. Phys. Chem.*, 1976, **80**, 2521.
23 A. Kulbida and A. Nosov, *J. Mol. Struct.*, 1992, **265**, 17.
24 W. J. Hehre, R. Ditchefield and J. A. Pople, *J. Chem. Phys.*, 1972, **56**, 2257.
25 R. Krishnan, J. S. Binkley, R. Seeger and J. A. Pople, *J. Chem. Phys.*, 1980, **72**, 4244.
26 M. J. Frisch, G. W. Trucks, M. Head-Gordon, P. M. W. Gill, M. W. Wong, J. B. Foresman, B. J. Johnson, H. B. Schlegel, M. A. Robb, E. S. Replogle, R. Gomperts, J. L. Andres, K. Raghavachari, J. S. Binkley, C. Gonzalez, R. L. Martin, D. J. Fox, D. J. Defrees, J. Baker, J. J. P. Stewart and J. A. Pople, GAUSSIAN92 (Revision C), Gaussian Inc., Pittsburgh, PA, 1992.
27 H. B. Schlegel, PhD Thesis, Queen's University Ontario, 1975.
28 M. D. G. Faria and R. Fausto, TRANSFORMER (version 1.0), Departamento de Química, Universidade de Coimbra, Portugal, 1990.
29 M. D. G. Faria and R. Fausto, BUILD-G and VIBRAT, Departamento de Química, Universidade de Coimbra, Portugal, 1990 (these programs incorporate several routines from programs GMAT and FPERT, H. Fuher, V. B. Kartha, K. G. Kidd, P. J. Krueger and H. H. Mantsch, *Natl. Res. Council Can. Bull.*, 1976, **15**, 1).
30 W. B. Person and J. H. Newton, *J. Chem. Phys.*, 1974, **61**, 1040.
31 W. B. Person, B. Ziller, J. D. Rogers and R. G. A. Maia, *J. Mol. Struct.*, 1982, **80**, 297.
32 A. J. Bowles, W. O. George and W. F. Maddams, *J. Chem. Soc.*, 1969, **B**, 810.
33 L. A. Carreira, *J. Phys. Chem.*, 1976, **80**, 1149.
34 J. De Smedt, F. Vanhouteghem, C. v. Alsenoy, H. J. Geise, B. v. der Veken and P. Coppens, *J. Mol. Struct.*, 1989, **195**, 227.
35 J. I. Kierns and R. F. Curl, *J. Chem. Phys.*, 1968, **48**, 3773.

36 R. Kewley, D. C. Hemphill and R. F. Curl, *J. Mol. Spectrosc.*, 1972, **44**, 443.
37 H. N. Voltrauer and R. H. Chwendeman, *J. Chem. Phys.*, 1971, **54**, 268.
38 J. R. Durig, R. J. Berry and P. Groner, *J. Chem. Phys.*, 1987, **87**, 6303.
39 P. Carmona and J. Moreno, *J. Mol. Struct.*, 1982, **82**, 177.
40 M. D. G. Faria, J. J. C. Teixeira-Dias and R. Fausto, *Vibrat. Spectrosc.*, 1991, **2**, 43.
41 M. D. G. Faria, J. J. C. Teixeira-Dias and R. Fausto, *Vibrat. Spectrosc.*, 1991, **2**, 107.
42 A. Kulbida and R. Fausto, *J. Chem. Soc., Faraday Trans.*, 1993, **89**, 4257.
43 J. J. C. Teixeira-Dias and R. Fausto, *J. Mol. Struct.*, 1986, **144**, 199.
44 R. Fausto and J. J. C. Teixeira-Dias, *J. Mol. Struct.*, 1986, **144**, 215; 225; 241.
45 R. Fausto and J. J. C. Teixeira-Dias, *J. Mol. Struct. (Theochem.)*, 1987, **150**, 381.
46 R. Fausto, F. P. S. C. Gil and J. J. C. Teixeira-Dias, *J. Chem. Soc., Faraday Trans.*, 1993, **89**, 3235.
47 P. J. Tonge, M. Pusztai, A. J. White, C. W. Wharton and P. R. Carey, *Biochemistry*, 1991, **29**, 4790.
48 R. Fausto and J. J. C. Teixeira-Dias, *J. Mol. Struct. (Theochem.)*, 1993, **101**, 123.
49 M. Gussoni, M. N. Ramos, C. Castiglioni and G. Zerbi, *Chem. Phys. Lett.*, 1987, **142**, 515.
50 M. N. Ramos, M. Gussoni, C. Castiglioni and G. Zerbi, *Chem. Phys. Lett.*, 1988, **151**, 397.
51 M. N. Ramos, C. Castiglioni, M. Gussoni and G. Zerbi, *Chem. Phys. Lett.*, 1990, **170**, 335.
52 R. Fausto, L. A. E. Batista de Carvalho, J. J. C. Teixeira-Dias and M. N. Ramos, *J. Chem. Soc., Faraday Trans.*, 1989, **85**, 1945.
53 T. Kar and A. B. Sannigrehi, *J. Mol. Struct.*, 1988, **165**, 47.
54 C. W. Kirn and M. Karplus, *J. Chem. Phys.*, 1964, **40**, 1374.
55 M. Gussoni, *J. Mol. Struct.*, 1986, **141**, 63.
56 C. Castiglioni, M. Gussoni and G. Zerbi, *J. Chem. Phys.*, 1985, **82**, 3534.
57 A. J. Bowles, W. O. George and D. B. Cunliffe-Jones, *J. Chem. Soc.*, 1970, **B**, 1070.
58 W. P. Hayes and C. J. Timmons, *Spectrochim. Acta, Part A*, 1968, **24**, 323.

Paper 5/00048C; *Received* 4*th January*, 1995